PRAMANA
— journal of
physics

Vol. 76, No. 1
January 2011
pp. 93–107

Next-to-next-leading order correction to 3-jet rate and event-shape distribution

MOHAMMAD EBRAHIM ZOMORRODIAN*, ALIREZA SEPEHRI, TOORAJ GHAFFARY and PARVIN ESLAMI

Department of Physics, Ferdowsi University of Mashhad, Mashhad 91775-1436, Khorasane, Razavi, Iran

*Corresponding author. E-mail: zomorrod@ferdowsi.um.ac.ir

MS received 25 January 2010; accepted 14 May 2010

Abstract. The hadronic events from the e^+e^- annihilation data at the centre-of-mass energies ranging from 60 to 197 GeV were studied. The AMY and OPAL Collaborations offered a unique opportunity to test QCD by measuring the energy dependence of different observables. The coupling constant, α_s, was measured by two different methods: first by employing the three-jet observables. Combining all the data, the value of as at next-to-next leading order (NNLO) was determined to be 0.117 $\pm$ 0.004(hard) $\pm$ 0.006(theo). Secondly, from the event-shape distributions, the strong coupling constant, α_s, was extracted at NNLO and it's evaluation was tested with the energy scale. The results were consistent with the running of α_s, expected from QCD predictions. Averaging over different observables, α_s was determined to be 0.115 $\pm$ 0.007(hard) $\pm$ 0.003(theo).

Keywords. Transverse momenta; three-jet rate; event shapes.

PACS No. 13.66.Bc

1. Introduction

Till three years ago, the precision of the strong coupling constant determined from the event shape data was not satisfactory largely due to the scale uncertainty of the perturbative NLO calculation. Recently, some papers reported the first calculations of NNLO corrections to event-shape variables and three-jet observables, and discussed their phenomenological impact [1,2].

Three-jet production at tree-level is induced by the decay of a virtual photon (or other neutral gauge boson) into a quark–antiquark–gluon final state. At higher orders, this process receives corrections from extra real or virtual particles. The individual partonic channels that contribute through to NNLO are cited in ref. [1]. For a given partonic final state, the event-shape observable **y** is computed according to the same definition as in the experiment, which is applied to partons instead of hadrons. At leading order, all three

final-state partons must be well separated from each other, such that **y** differs from the trivial two-parton limit. At NLO, up to four partons can be present in the final-state, two of which can be clustered together, whereas at NNLO, the final state consists of up to five partons, and as many as three partons can be clustered together. When more partons are there in the final state, one expects a better matching between theory and experiment [3].

The data from e^+e^- annihilation provide us with one of the cleanest ways of probing our quantitative understanding of QCD giving us an opportunity to measure the strong coupling between quarks and gluons. Three-jet production cross-sections and the related event-shape distributions in the e^+e^- annihilation processes are classic hadronic observables which can be measured very accurately and provide an ideal testing ground to understand strong interactions.

Jet observables in electron–positron annihilation can be used to find the value of the strong coupling constant $\alpha_{\rm s}$ [4–6]. This applies in particular to three-jet observables, where the leading-order parton process is proportional to $\alpha_{\rm s}$. In order to extract the numerical value from the AMY data, precise theoretical calculations are necessary, calling for the next-to-next-to-leading order (NNLO) calculation.

Many 'event shape' observables were devised which provided a convenient way of characterizing the main features of such events. Analytic QCD predictions of the distributions of several of these event-shape observables are given in [7], which can be used to determine the crucial free parameter of the QCD – the coupling strength $\alpha_{\rm s}$ at NNLO.

In this paper we separated two- and three-jets events using the jet clustering algorithm introduced by the JADE group [8,9]. Using the newly computed NNLO corrections to three-jet rates and event-shape variables, we performed a new extraction of $\alpha_{\rm s}$ from the data on the standard set of three-jet observable and five event-shape variables, by using the AMY [10] and OPAL [7–11] data at the centre-of-mass energies ranging from 60 GeV to 197 GeV. The last section includes summary and conclusions.

2. JADE algorithm

We separated two- and three-jet events by employing the jet clustering algorithm introduced by the JADE group [8]. In this algorithm the scaled mass spread defined as $Y_{ij} = m_{ij}^2/E_{\rm vls}^2$ with $m_{ij}^2 = 2E_iE_j(1-\cos\theta_{ij})$ is calculated for each pair of particles in the event. If the smallest of the Y_{ij} values is less than a parameter $Y_{\rm cut}$, the corresponding pair of particles is combined into a cluster by summing the four momenta. This process is repeated, using all combinations of clusters and remaining particles, until all the Y_{ij} values exceed $Y_{\rm cut}$. The clusters remaining at this stage are defined as the jets.

The distribution of jet multiplicities obtained by these clustering algorithms depends on the jet defining parameter $Y_{\rm cut}$. For small $Y_{\rm cut}$, many jets are found because of the hadronization of fluctuation process, whereas for large $Y_{\rm cut}$, mostly two jet events are found and the $q\bar{q}g$-events are not resolved. However, Monte Carlo studies show that there is a range of cluster parameters, for which QCD effects can be resolved and the fragmentation effects are sufficiently small. In the following, $Y_{\rm cut} = 0.04$ was used which was found to be a reasonable cut [8].

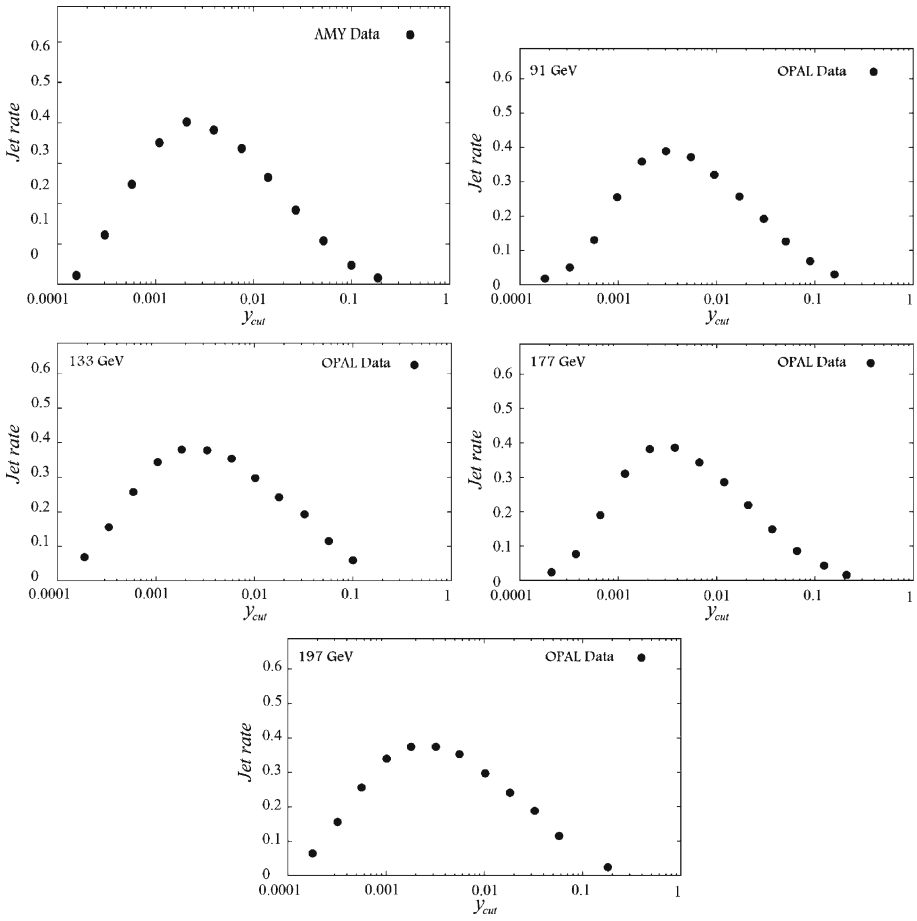

Figure 1. Three jet fraction for different $Y_{\rm cut}$s. The data are from refs [7,10,11].

In figure 1, we show three-jet fraction for different $Y_{\rm cut}$s. The decrease of the 3-jet rate at large $Y_{\rm cut}$ is clearly visible. Our results on AMY and OPAL data [7,10,11] are completely consistent with the results obtained by the JADE scheme [8,9].

3. Three-jet observables at NNLO

Up to now, the precision of the strong coupling constant determined from event-shape data has been limited largely by the scale uncertainty of the perturbative NLO calculation [1,2,12]. In this paper, we report the first calculation of NNLO corrections to the 3-jet cross-section and related event-shape variables. The knowledge of the NNLO corrections

to the event-shape distributions has important phenomenological impact on the extraction of strong coupling constant from AMY and OPAL data [7,10,11].

The α_s^3 corrections for the three-jet production was calculated using a recently developed parton-level event-generator program EERAD3 [13]. This contains the relevant matrix elements with up to five external partons. Besides the explicit infrared divergences from the loop integrals, the four-parton and five-parton contributions yield infrared divergent contributions if one or two of the final-state partons become collinear or soft. To extract these infrared divergences and combine them with the virtual corrections, the antenna subtraction method [14] was extended to NNLO level [15] and related event-shape variables [16,17] into EERAD3.

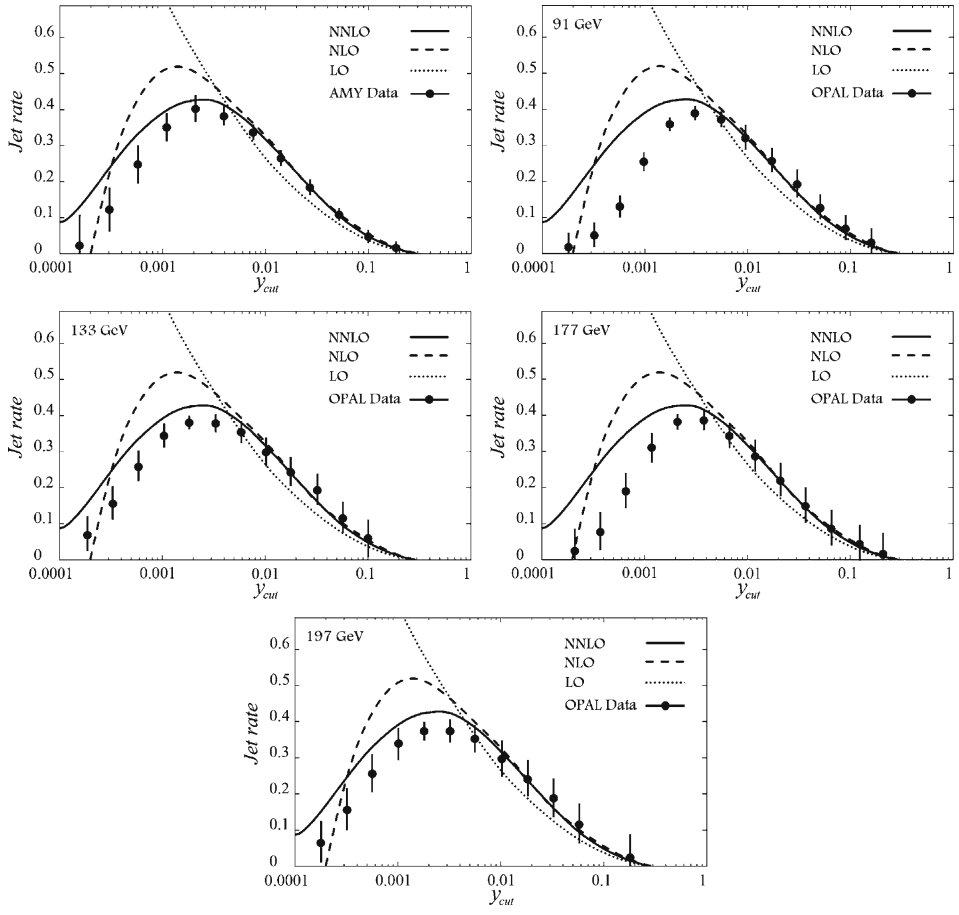

Figure 2. The scale variation of the three-jet rate with the JADE jet algorithm. The data are from refs [7,10,11] and the model is from ref. [12].

Table 1. $\alpha_{\rm s}$ values for different centre-of-mass energies from 60 to 197 GeV.

	60 GeV	91 GeV	133 GeV	177 GeV	197 GeV
$\alpha_{\rm s}$	0.123	0.119	0.112	0.104	0.105
	$\pm$ 0.003(hadr)	$\pm$ 0.006(hadr)	$\pm$ 0.005(hadr)	$\pm$ 0.004(hadr)	$\pm$ 0.007(hadr)
	$\pm$ 0.004(theo)	$\pm$ 0.005(theo)	$\pm$ 0.003(theo)	$\pm$ 0.007(theo)	$\pm$ 0.002(theo)

The three-jet cross-section is expanded as [12]

$$\frac{\sigma_{\text{3-jet}}}{\sigma_{\rm tot}} = \frac{\alpha_{\rm s}}{2\pi} A_{\text{3-jet}} + \left(\frac{\alpha_{\rm s}}{2\pi}\right)^2 B_{\text{3-jet}} + \left(\frac{\alpha_{\rm s}}{2\pi}\right)^3 C_{\text{3-jet}}, \tag{4}$$

where σ_0 is the LO cross-section for $e^+e^- \rightarrow$ hadrons. The coefficients $A_{\text{3-jet}}$, $B_{\text{3-jet}}$ and $C_{\text{3-jet}}$ are calculated for $\mu^2 = Q^2$ [12]. The measured three-jet cross-sections are shown in figure 2 for both AMY and OPAL data.

As the figures indicate, by comparing our measured values with perturbation theory in different orders, we observed that the agreement for each of the jet rates became systematically better as the order of perturbation theory increased. By fitting our data with eq. (4) the strong coupling constant $\alpha_{\rm s}$ can be derived. The values of $\alpha_{\rm s}$ are presented in table 1 and also in figure 3. Systematic uncertainties arise from the modelling of the hadronization. These were estimated using NNLO model. The NNLO model employs a different hadronization model, for determining the theoretical prediction correction factor. The fit-related systematic variation accounted for the uncertainty due to the dependence of the fixed order and resummed predictions on the renormalization scale, x_μ, where $x_\mu = \mu/\sqrt{s}$. The value of x_μ could be either 0.5 or 1. The largest deviation from the standard fit value was taken as the contribution to the systematic error representing

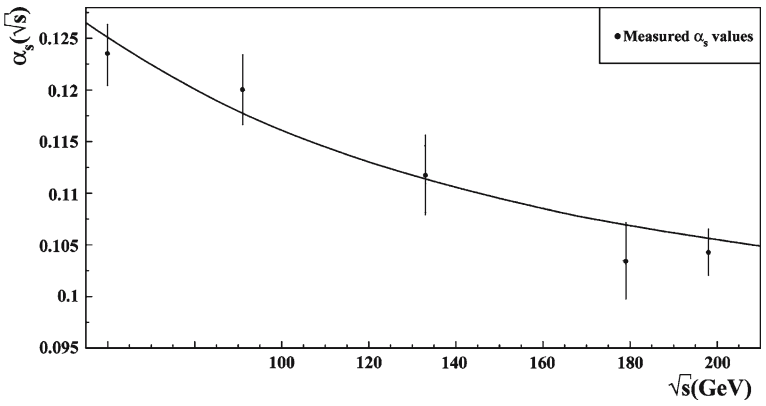

Figure 3. The plot of $\alpha_{\rm s}$ as a function of the centre-of-mass energy for three-jet rate.

renormalization scale uncertainty. The standard value of α_s was estimated by comparing theory with data using the value of $x_\mu = 1$.

4. Event shapes in perturbation theory [1–3]

The perturbative expansion for the distribution of a generic observable **y** up to NNLO at centre-of-mass energy $\sqrt{s}$ for renormalization scale $\mu^2 = s$ and $\alpha_s = \alpha_s(\sqrt{s})$ is given by

$$\frac{1}{\sigma_{\rm had}}\frac{\mathrm{d}\sigma}{\mathrm{d}y} = \left(\frac{\alpha_s}{2\pi}\frac{\mathrm{d}\bar{A}}{\mathrm{d}y} + \left(\frac{\alpha_s}{2\pi}\right)^2\frac{\mathrm{d}\bar{B}}{\mathrm{d}y}\right) + \left(\frac{\alpha_s}{2\pi}\right)^3\frac{\mathrm{d}\bar{C}}{\mathrm{d}y} + O\big(\alpha_s^4\big). \tag{5}$$

Here the event-shape distribution is normalized to the total hadronic cross-section $\sigma_{\rm had}$.

With the assumption of massless quarks, then at NNLO we have,

$$\sigma_{\rm had} = \sigma\left(1 + \frac{3}{2}C_F\left(\frac{\alpha_s}{2\pi}\right) + K_2\left(\frac{\alpha_2}{2\pi}\right)^2 + O\big(\alpha_s^3\big)\right), \tag{6}$$

where the Born cross-section for $e^+e^- \to q\bar{q}$ is

$$\sigma_0 = \frac{4\pi\alpha}{3s}Ne_q^2. \tag{7}$$

The constant K_2 is given by

$$K_2 = \frac{1}{4}\left[-\frac{3}{2}C_F^2 + C_FC_A\left(\frac{123}{2} - 44\varsigma_3\right) + C_FT_RN_F(-22 + 16\varsigma_3)\right], \tag{8}$$

where $\varsigma_3 = 1.202056903\ldots$ and the QCD colour factors are

$$C_A = N, \quad C_F = \frac{N^2-1}{2N}, \quad T_R = \frac{1}{2} \tag{9}$$

for $N = 3$ colours and N_F light quark flavours.

In practice, we compute the perturbative coefficients A, B and C, which are all normalized to σ_0:

$$\frac{1}{\sigma_0}\frac{\mathrm{d}\sigma}{\mathrm{d}y} = \left(\frac{\alpha_s}{2\pi}\right)\frac{\mathrm{d}A}{\mathrm{d}y} + \left(\frac{\alpha_s}{2\pi}\right)^2\frac{\mathrm{d}B}{\mathrm{d}y} + \left(\frac{\alpha_s}{2\pi}\right)^3\frac{\mathrm{d}C}{\mathrm{d}y} + O\big(\alpha_s^4\big). \tag{10}$$

A, B and C however are related to $\bar{A}$, $\bar{B}$ and $\bar{C}$ as

$$\begin{aligned}\bar{A} &= A,\\ \bar{B} &= B - \frac{3}{2}C_FA,\\ \bar{C} &= C - \frac{3}{2}C_FB + \left(\frac{9}{4}C_F^2 - K_2\right)A.\end{aligned} \tag{11}$$

These coefficients are computed at a renormalization scale fixed to the centre-of-mass energy, and depend therefore only on the value of the observable y. They explicitly include only QCD corrections with non-singlet quark couplings and are therefore independent of electroweak couplings. At $O(\alpha_s^2)$, these amount to the full corrections, while the $O(\alpha_s^3)$

corrections also receive a pure-singlet contribution. This pure-singlet contribution arises from the interference of diagrams where the external gauge boson couples to different quark lines. In four-jet observables at $O(\alpha_s^3)$, these singlet contributions were found to be extremely small [18].

The QCD coupling constant evolves according to the renormalization group equation, which is to NNLO:

$$\mu^2 \frac{\mathrm{d}\alpha_s(\mu)}{\mathrm{d}\mu^2} = -\alpha_s(\mu)\left[\beta_0\left(\frac{\alpha_s(\mu)}{2\pi}\right) + \beta_1\left(\frac{\alpha_s(\mu)}{2\pi}\right)^2 + \beta_2\left(\frac{\alpha_s(\mu)}{2\pi}\right)^3 + O\big(\alpha_s^4\big)\right] \tag{12}$$

with the MS-scheme coefficients

$$\begin{aligned}
\beta_0 &= \frac{11C_A - 4T_R N_F}{6} \\
\beta_1 &= \frac{17C_A^2 - 10C_A T_R N_F - 6C_F T_R N_F}{6}, \\
\beta_2 &= \frac{1}{432}(2857C_A^3 + 108C_F^2 T_R N_F - 1230C_F C_A T_R N_F \\
&\quad -2830C_A^2 T_R N_F + 264C_F T_R^2 N_F^2 + 316C_A T_R^2 N_F^2).
\end{aligned} \tag{13}$$

Equation (12) is solved by introducing $\Lambda_{\mathrm{MS}}^{N_F}$ as integration constant with $L = 2\,\log(\mu/\Lambda_{\mathrm{MS}}^{N_F})$, yielding the running coupling constant:

$$\alpha_s(\mu) = \frac{2\pi}{\beta_0 L}\left(1 - \frac{\beta_1}{\beta_0^2}\frac{\log L}{L} + \frac{1}{\beta_0^2 L^2}\left(\frac{\beta_1^2}{\beta_0^2}\big(\log^2 L - \log L - 1\big) + \frac{\beta_2}{\beta_0}\right)\right). \tag{14}$$

In terms of the running coupling α_s, the NNLO (non-singlet) expression for the event-shape distributions becomes

$$\begin{aligned}
\frac{1}{\sigma_{\mathrm{had}}}\frac{\mathrm{d}\sigma}{\mathrm{d}y}(s,\mu^2,y) &= \left(\frac{\alpha_s(\mu)}{2\pi}\frac{\mathrm{d}\bar{A}}{\mathrm{d}y} + \left(\frac{\alpha_s(\mu)}{2\pi}\right)^2\right)\left(\frac{\mathrm{d}\bar{B}}{\mathrm{d}y} + \frac{\mathrm{d}\bar{A}}{\mathrm{d}y}\beta_0 \log\frac{\mu^2}{s}\right) \\
&\quad + \left(\frac{\alpha_s(\mu)}{2\pi}\right)^3\left(\frac{\mathrm{d}\bar{C}}{\mathrm{d}y} + 2\frac{\mathrm{d}\bar{B}}{\mathrm{d}y}\beta_0 \log\frac{\mu^2}{s}\right. \\
&\quad \left. + \frac{\mathrm{d}A}{\mathrm{d}y}\left(\beta_0^2 \log^2\frac{\mu^2}{s} + \beta_1 \log\frac{\mu^2}{s}\right)\right) + O(\alpha_s^4).
\end{aligned} \tag{15}$$

Besides explicit infrared divergences from the loop integrals, the four-parton and five-parton contributions yield infrared divergent contributions if one or two of the final-state partons become collinear or soft. In order to extract these infrared divergences and combine them with the virtual corrections, the antenna subtraction method [19] was extended to NNLO level [20] and implemented for $e^+e^- \to 3$ jets and related event-shape variables [21]. The analytical cancellation of all infrared divergences serves as a

very strong check on the implementation. EERAD3 yields the perturbative A, B and C coefficients as histograms for all infrared-safe event-shape variables related to three-particle final states at leading order. As a cross-check, A and B have also been obtained from an independent integration [22] of the NLO matrix elements [23], showing excellent agreement. While A and B can be computed to very high numerical accuracy, the computation of C is so CPU-intensive that we could obtain only results with numerical integration errors of typically a few per cent [1].

5. Event-shape variable

The properties of hadronic events can be described by a set of event-shape observables. These can be used to characterize the distribution of particles in an event as 'pencil-like', planar, spherical, etc. They can be computed by either using the measured charged particles and calorimeter clusters, or by using the true hadrons or partons in simulated events. The following event shapes are considered here:

(a) *Thrust, T* [24]

The global event-shape variable thrust is defined as

$$T = \max\left(\frac{\sum \vec{p}_i \cdot \vec{n}}{\sum |\vec{p}_i|}\right), \tag{16}$$

where $\vec{p}_i$ is the momentum vector of particle i. The thrust axis $\vec{n}$ is the unit vector which maximizes the above expression. The value of the thrust can vary between 0.5 and 1.0.

(b) *Jet broadening*, B_{W} *and* B_{T} [25]

Taking a plane perpendicular to $\vec{n}_{\mathrm{T}}$ through the coordinate origin, one defines two event hemispheres $H_{1,2}$. In each of them, one determines the hemisphere broadening:

$$B_i = \frac{\sum_{k\in H_i} |\vec{p}_k \times \vec{n}_{\mathrm{T}}|}{2\sum_k |\vec{p}_k|}. \tag{17}$$

The wide and total jet broadening are then defined as

$$B_{\mathrm{W}} = \max(B_1, B_2), \tag{18}$$

$$B_{\mathrm{T}} = B_1 + B_2. \tag{19}$$

(c) *The C-parameter* [26]

The C-parameter is derived from the eigenvalues of the linearized momentum tensor

$$\theta^{\alpha/3} = \frac{1}{\sum_k |\vec{p}_k|}\sum_k \frac{P_k^\alpha P_k^\beta}{|\vec{P}_k|}, \quad \alpha,\beta = 1,2,3 \tag{20}$$

which has three eigenvalues λ_i. These eigenvalues are used to construct the C-parameter:

$$C = 3(\lambda_1\lambda_2 + \lambda_2\lambda_3 + \lambda_3\lambda_1). \tag{21}$$

This definition is equivalent to

$$C = 3(\theta^{11}\theta^{22} + \theta^{22}\theta^{33} + \theta^{33}\theta^{11} - \theta^{12}\theta^{12} - \theta^{23}\theta^{23} - \theta^{31}\theta^{31}). \tag{22}$$

6. Determination of α_s using event-shape distributions and calculating uncertainties

In §4, eq. (15) is the perturbative expansion for the distribution of a generic observable **y** up to NNLO, for the renormalization scale μ^2 [1].

The coefficients A, B and C were computed for several event-shape variables [1,2,12, 27,28]. The calculation was carried out using a newly developed parton-level event generator programme EERAD3 which contained the relevant matrix elements with up to five external partons [29–32]. The measured normalized differential cross-sections, for each of the four event shapes are shown in figures 4–7 for 60 to 197 GeV centre-of-mass energies. As the figures indicate, our real data are consistent with NNLO compared to NLO or

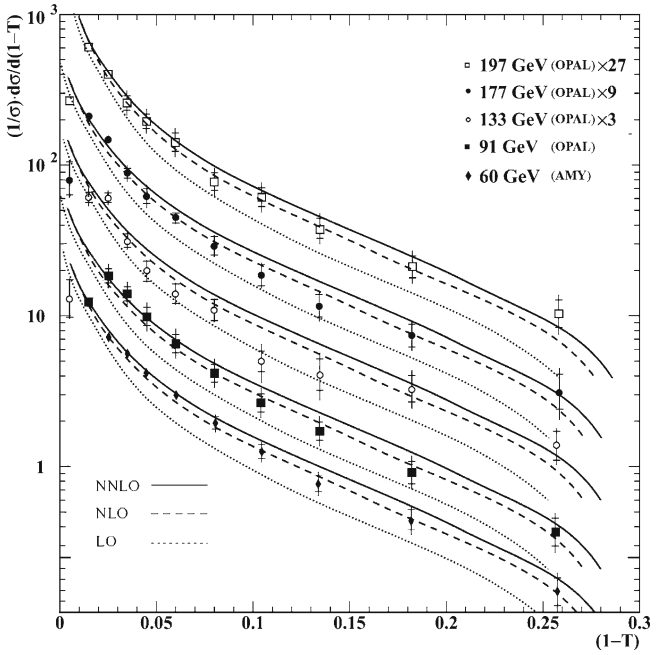

Figure 4. The thrust distribution at LO (dotted line), NLO (dashed line) and NNLO (solid line) compared to experimental data from AMY and OPAL for $Q = 60$–197 GeV. The data are from refs [7,10,11] and the model is from refs [1–3,12].

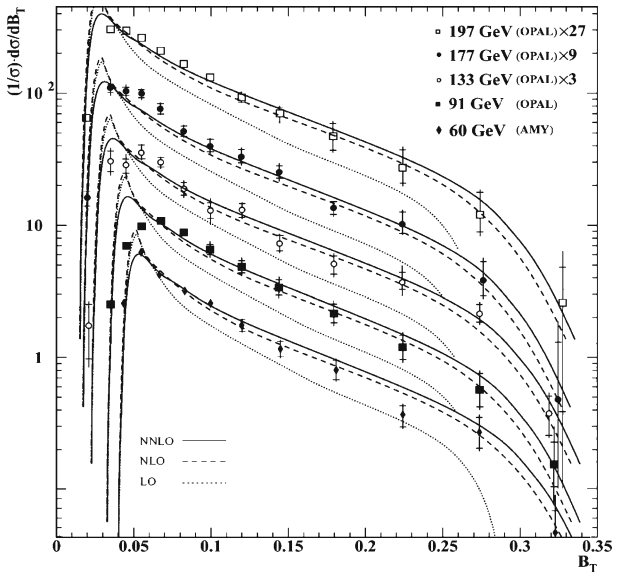

Figure 5. Total jet broadening distribution at LO (dotted line), NLO (dashed line) and NNLO (solid line) compared to experimental data from AMY and OPAL for $Q = 60$–197 GeV. The data are from refs [7,10,11] and the model is from refs [1–3,12].

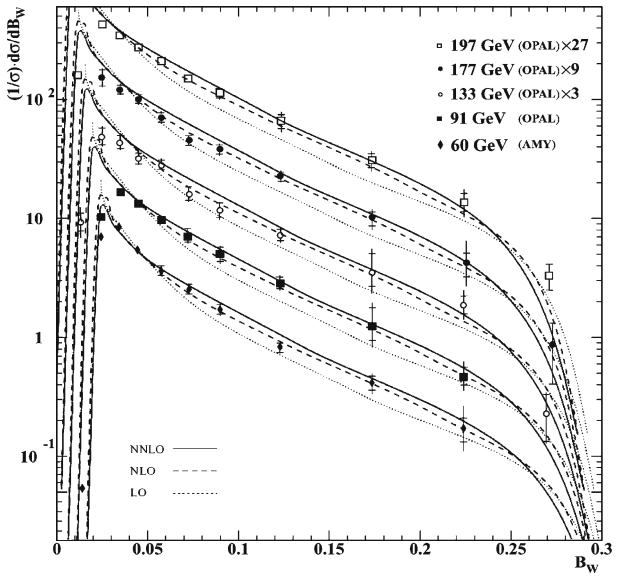

Figure 6. Wide jet broadening distribution at LO (dotted line), NLO (dashed line) and NNLO (solid line) compared to experimental data from AMY and OPAL for $Q = 60$–197 GeV. The OPAL data are from refs [7,10,11] and the model is from refs [1–3,12].

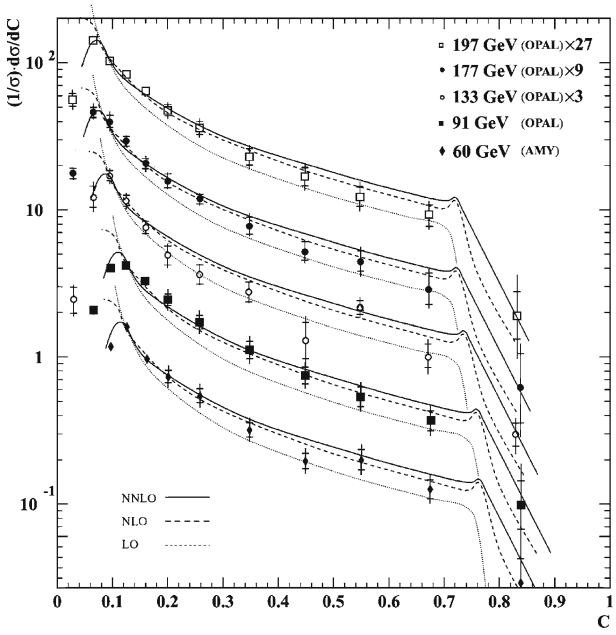

Figure 7. C parameter distribution at LO (dotted line), NLO (dashed line) and NNLO (solid line) compared to experimental data from AMY and OPAL for $Q = 60$–197 GeV. The OPAL data are from refs [7,10,11] and the model is from refs [1–3,12].

LO calculations, because it involves higher-order terms in QCD calculations. The value of $\alpha_{\rm s}$ can be estimated by fitting the data with eq. (15).

In our calculations, two other sources of errors were considered.

(1) When comparing QCD with the data, it is necessary to correct for the effects of hadronization. The uncertainty associated with this hadronization correction was assessed using NNLO model. The larger change in $\alpha_{\rm s}$ resulting from these two alternatives was taken to define the error. It should be noted that these models have already been tuned to similar data to those used here, and hence we adopted this, arguably conservative, prescription for assessing the error.

(2) The theoretical error, associated with the missing higher-order terms in the theory, has traditionally been assessed by varying the renormalization scale factor, x_μ. In all these results, the uncertainty due to the choice of the renormalization scale $x_\mu = \mu/\sqrt{s}$ yields a large contribution to the total error. Consequently, missing higher orders, whose effects on the values of the coupling are assessed by varying x_μ, are still important. The fitted values for $\alpha_{\rm s}$ change considerably for different choices of the scale. This is demonstrated for the C parameter, in figure 8. The plot shows the strong dependence of the fitted $\alpha_{\rm s}$ on the renormalization scale factor x_μ. The real value of $\alpha_{\rm s}$ was estimated by comparing the theory with data using the minimum of χ^2 in this figure, such that wherever χ^2 was

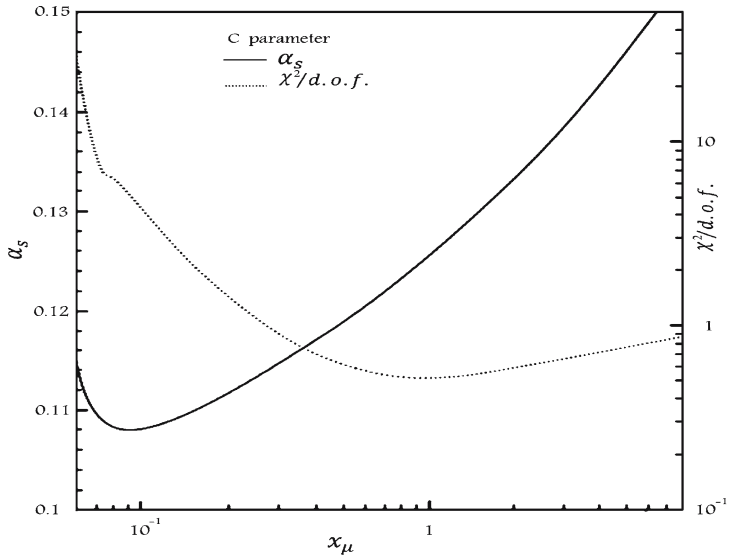

Figure 8. The plot showing the residual dependence of the fitted value of $\alpha_{\rm s}$ and uncertainty χ^2 on the renormalization factor.

minimum, it's corresponding $\alpha_{\rm s}$ value became our real strong coupling constant. In table 2 we present the values of $\alpha_{\rm s}$ for different observables on each available energy. Averaging over different observables for different energies, the values of $\alpha_{\rm s}$ are indicated in figure 9.

Table 2. $\alpha_{\rm s}$ values for different event shapes at 60–197 GeV.

	T	$B_{\rm T}$	$B_{\rm W}$	C
$\alpha_{\rm s}(60)$	0.123	0.122	0.127	0.126
	$\pm$ 0.003(hadr)	$\pm$ 0.005(hadr)	$\pm$ 0.002(hadr)	$\pm$ 0.006(hadr)
	$\pm$0.005(theo)	$\pm$0.007(theo)	$\pm$0.003(theo)	$\pm$0.008(theo)
$\alpha_{\rm s}(90)$	0.119	0.118	0.116	0.115
	$\pm$ 0.005(hadr)	$\pm$ 0.007(hadr)	$\pm$ 0.005(hadr)	$\pm$ 0.003(hadr)
	$\pm$0.001(theo)	$\pm$0.005(theo)	$\pm$0.007(theo)	$\pm$0.006(theo)
$\alpha_{\rm s}(133)$	0.114	0.111	0.109	0.107
	$\pm$ 0.004(hadr)	$\pm$ 0.004(hadr)	$\pm$ 0.006(hadr)	$\pm$ 0.009(hadr)
	$\pm$0.002(theo)	$\pm$0.008(theo)	$\pm$0.004(theo)	$\pm$0.001(theo)
$\alpha_{\rm s}(177)$	0.106	0.109	0.107	0.113
	$\pm$ 0.003(hadr)	$\pm$ 0.003(hadr)	$\pm$ 0.005(hadr)	$\pm$ 0.004(hadr)
	$\pm$0.005(theo)	$\pm$0.007(theo)	$\pm$0.002(theo)	$\pm$0.008(theo)
$\alpha_{\rm s}(197)$	0.110	0.107	0.109	0.112
	$\pm$ 0.002(hadr)	$\pm$ 0.004(hadr)	$\pm$ 0.007(hadr)	$\pm$ 0.008(hadr)
	$\pm$0.002(theo)	$\pm$0.005(theo)	$\pm$0.004(theo)	$\pm$0.007(theo)

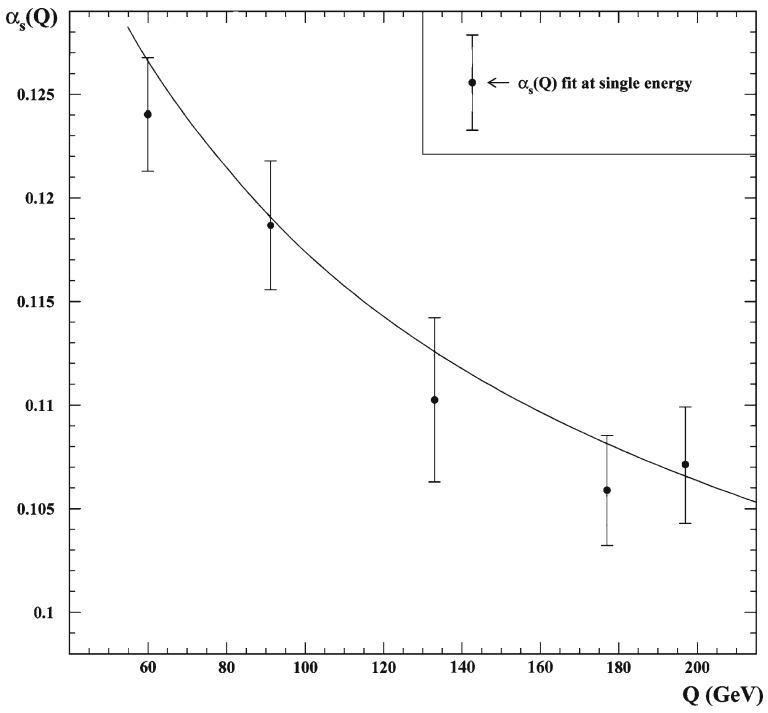

Figure 9. The running of $\alpha_{\rm s}$ as a function of the centre-of-mass energy.

7. Summary and conclusions

In this paper we have presented measurements of the three-jet rate event shapes for hadronic events produced at AMY and OPAL at the centre-of-mass energies between 60 and 197 GeV. The predictions of the NNLO are found to be in general agreement with the measured distributions. In general, NNLO provides the best description of the data and LO the worst. The coupling constant, $\alpha_{\rm s}$, was measured by two different methods: (1) by employing the three-jet observables. The variation of $\alpha_{\rm s}$ with energy scale over a range of 60 to 197 GeV was found to be in accordance with the expectations of QCD. (2) From the event-shape distributions. We extracted the strong coupling constant, $\alpha_{\rm s}$, and tested it's evaluation with energy scale. The results are consistent with the running of $\alpha_{\rm s}$, expected from QCD predictions.

References

[1] A Gehrmann-De Ridder, T Gehrmann, E W N Glover and G Heinrich, *J. High Energy Phys.* **0712**, 094 (2007)
G Dissertori, A Gehrmann-De Ridder, T Gehrmann, E W N Glover, G Heinrich and H Stenzel (Giessen U), *Phys. Rev. Let.* **104**, 072002 (2010), arXiv:0910.4283[hep-ph]

[2] G Dissertori, A Gehrmann-De Ridder, T Gehrmann, E W N Glover, G Heinrich and H Stenzel, *J. High Energy Phys.* **0802**, 040 (2008)
Stefan Weinzierl, *J. High Energy Phys.* **0906**, 041 (2009)
[3] E W N Glover, *Nucl. Phys. Proc. Suppl.* **116**, 3 (2003), arXiv:hep-ph/0211412
[4] O Biebel, *Phys. Rep.* **340**, 165 (2001)
[5] S Kluth, *Rep. Prog. Phys.* **69**, 1771 (2006), hepex/0603011
[6] S Bethke, *Prog. Part. Nucl. Phys.* **58**, 351 (2007), hepex/0606035
[7] OPAL Collaboration: G Abbiendi *et al*, *Eur. Phys. J.* **C45**, 547 (2006)
OPAL Collaboration: G Abbiendi *et al*, *Eur. Phys. J.* **C40**, 287 (2005)
OPAL Collaboration: *Eur. Phys. J.* **C53**, 21 (2008)
The OPAL Collaboration: *Phys. Lett.* **B658**, 185 (2008)
OPAL Collaboration: *Eur. Phys. J.* **C47**, 295 (2006)
OPAL Collaboration: *Phys. Lett.* **B609**, 212 (2005)
[8] JADE and OPAL Collaboration: G Abbiendi *et al*, *Eur. Phys. J.* **C17**, 19 (2000)
[9] JADE Collaboration: W Bartel *et al*, *Z. Phys.* **C33**, 23 (1986)
[10] AMY Collaboration: K B Lee *et al*, *Phys. Lett.* **B 313**, 469 (1993)
Li *et al*, *Phys. Rev.* **D41**, 2675 (1990)
VENUS Collaboration: K Abe *et al*, *Phys. Lett.* **B240**, 232 (1990); *Phys. Lett.* **B234**, 382 (1990); *Phys. Lett.* **B232**, 425 (1989); *Phys. Rev. Lett.* **66**, 280 (1991); *Phys. Lett.* **B246**, 297 (1990)
AMY Collaboration, *Phys. Lett.* **B325**, 248 (1994)
AMY Collaboration: *Phys. Lett.* **B313**, 469 (1993)
JADE Collaboration: Movilla-Fernandez *et al*, *Eur. Phys. J.* **C1**, 461 (1998)
[11] OPAL Collaboration: *Eur. Phys. J.* **C40**, 287 (2005)
OPAL Collaboration: Acton *et al*, *Zeit. Phys.* **C55**, 1 (1992)
OPAL Collaboration: Ackerstaff *et al*, *Zeit. Phys.* **C72**, 191 (1996)
OPAL Collaboration: Ackerstaff *et al*, *Zeit. Phys.* **C75**, 193 (1997)
L3 Collaboration: Achard *et al*, *Phys. Rep.* **399**, 71 (2004)
OPAL Collaboration: G Abbiendi *et al*, *Eur. Phys. J.* **C45**, 547 (2006)
DELPHI Collaboration: Abreu *et al*, *Zeit. Phys.* **C73**, 229 (1997); *J. High Energy Phys.* **0712**, 094 (2007)
[12] Stefan Weinzierl, *J. High Energy Phys.* **0906**, 041 (2009)
Stefan Weinzierl, *Phys. Rev. Lett.* **101**, 162001 (2008)
Stefan Weinzierl, *J. High Energy Phys.* **0907**, 009 (2009)
G Dissertori, A Gehrmann-De Ridder, T Gehrmann, E W N Glover, G Heinrich and H Stenzel, *Nucl. Phys. Proc. Suppl.* **183**, 2 (2008)
[13] A Gehrmann-De Ridder, T Gehrmann, E W N Glover and G Heinrich, *J. High Energy Phys.* **0711**, 058 (2007)
G Dissertori, A Gehrmann-De Ridder, T Gehrmann, E W N Glover, G Heinrich and H Stenzel, *Nucl. Phys. Proc. Suppl.* **183**, 2 (2008)
[14] D A Kosower, P*hys. Rev.* **D 57**, 5410 (1998); *Phys. Rev.* **D71**, 045016 (2005)
J Campbell, M A Cullen and E W N Glover, *Eur. Phys. J.* **C9**, 245 (1999)
A Daleo, T Gehrmann and D Matre, *J. High Energy Phys.* **0704**, 016 (2007)
[15] A Gehrmann-De Ridder, T Gehrmann and E W N Glover, *J. High Energy Phys.* **0509**, 056 (2005); *Phys. Lett.* **B612**, 36 (2005); **612**, 49 (2005)
[16] A Gehrmann-De Ridder, T Gehrmann, E W N Glover and G Heinrich, *Phys. Rev. Lett.* **100**, 172001 (2008)
[17] A Gehrmann-De Ridder, T Gehrmann, E W N Glover and G Heinrich, *Phys. Rev. Lett.* **99**, 132002 (2007); *J. High Energy Phys.* **0712**, 094 (2007)

[18] L J Dixon and A Signer, *Phys. Rev. Lett.* **78**, 811 (1997), hep-ph/9609460; *Phys. Rev.* **D56**, 4031 (1997), hep-ph/9706285
[19] D A Kosower, *Phys. Rev.* **D57**, 5410 (1998), hep-ph/9710213; *Phys. Rev.* **D71**, 045016 (2005), hep-ph/0311272
J Campbell, M A Cullen and E W N Glover, *Eur. Phys. J.* **C9**, 245 (1999), hep-ph/9809429
[20] A Gehrmann-De Ridder, T Gehrmann and E W N Glover, *J. High Energy Phys.* **0509**, 056 (2005), hep-ph/0505111; *Nucl. Phys.* **B691**, 195 (2004), hep-ph/0403057; *Phys. Lett.* **B612**, 36 (2005), hep-ph/0501291; **612**, 49 (2005), hep-ph/0502110
[21] A Gehrmann-De Ridder, T Gehrmann, E W N Glover and G Heinrich, *J. High Energy Phys.* **0711**, 058 (2007), arXiv:0710.0346
[22] Z Kunszt and P Nason, in *Z Physics at LEP 1*, CERN Yellow Report 89-08, Vol. 1, p. 373
S Catani and M H Seymour, *Phys. Lett.* **B378**, 287 (1996), hep-ph/9602277
[23] R K Ellis, D A Ross and A E Terrano, *Nucl. Phys.* **B178**, 421 (1981)
[24] S Brandt, C Peyrou, R Sosnowski and A Wroblewski, *Phys. Lett.* **12**, 57 (1964)
E Farhi, *Phys. Rev. Lett.* **39**, 1587 (1977)
[25] P E L Rakow and B R Webber, *Nucl. Phys.* **B191**, 63 (1981)
S Catani, G Turnock and B R Webber, *Phys. Lett.* **B295**, 269 (1992)
[26] G Parisi, *Phys. Lett.* **B74**, 65 (1978)
J F Donoghue, F E Low and S Y Pi, *Phys. Rev.* **D20**, 2759 (1979)
[27] A Gehrmann-De Ridder, T Gehrmann, E W N Glover and G Heinrich, *Phys. Rev. Lett.* **99**, 132002 (2007), arXiv:0707.1285
[28] A Gehrmann-De Ridder, T Gehrmann, E W N Glover and G Heinrich, *J. High Energy Phys.* **0712**, (2007)
[29] L W Garland, T Gehrmann, E W N Glover, A Koukoutsakis and E Remiddi, *Nucl. Phys.* **B627**, 107 (2002), hep-ph/0112081; **642**, 227 (2002), hep-ph/0206067
[30] S Moch, P Uwer and S Weinzierl, *Phys. Rev.* **D66**, 114001 (2002), hep-ph/0207043
[31] E W N Glover and D J Miller, *Phys. Lett.* **B396**, 257 (1997), hep-ph/9609474
Z Bern, L J Dixon, D A Kosower and S Weinzierl, *Nucl. Phys.* **B489**, 3 (1997), hep-ph/9610370
J M Campbell, E W N Glover and D J Miller, *Phys. Lett.* **B409**, 503 (1997), hep-ph/9706297
Z Bern, L J Dixon and D A Kosower, *Nucl. Phys.* **B513**, 3 (1998), hep-ph/9708239.094 [arXiv:0711.4711]
[32] K Hagiwara and D Zeppenfeld, *Nucl. Phys.* **B313**, 560 (1989)
F A Berends, W T Giele and H Kuijf, *Nucl. Phys.* **B321**, 39 (1989)
N K Falck, D Graudenz and G Kramer, *Nucl. Phys.* **B328**, 317 (1989)